Characterization of Chicken-Derived Genotype VII Newcastle Disease Virus Isolates from Northwest China

Xinxin Qiu[1,2], Yanqing Jia[2], Zhencang Zhang[2], Xianglin Fo[2] and Wenhui Wang[1]

[1]College of Veterinary Medicine, Gansu Agricultural University, Lanzhou, Gansu 730070, China
[2]Department of animal engineering/Shaanxi engineering research center of the prevention and control for animal disease, Yangling Vocational & Technical College, Yangling, Shaanxi Province 712100, China

Newcastle disease virus (NDV) threatens global poultry production, with genotype VII the most prevalent strain in China. However, little information is available regarding viral multiplication and pathogenicity based inoculation route. The objectives of this study were to sequence NDV VII isolates and to analyze their biological characteristics in detail. A total of 86 oral and cloacal swabs were collected from Shaanxi and Gansu provinces in northwest China. Identification of genotype VII NDV based on the M gene was performed by qPCR. Viral multiplication and pathogenicity were assessed as a function of route of infection. We observed increased morbidity and mortality using intravenous injection, whereas intranasal, intraocular, and cloacal infections resulted in slower progression and milder clinical disease, with viral proliferation obvious in different tissues. These results provide an important basis for the clinical control and prevention of NDV epidemics in poultry.

Introduction

Newcastle disease virus (NDV) belongs to the genus *Avulavirus* of the family *Paramyxoviridae* and causes Newcastle disease, which has been prevalent worldwide since 1926 (Gao et al., 2019; Wang et al., 2021). NDV has strong infectivity, spreads rapidly, is associated with high morbidity and fatality, and causes multiple diseases in birds. Based on mean death time (MDT), intracerebral pathogenicity index (ICPI), and intravenous pathogenicity index (IVPI), NDV strains have been characterized as velogenic, mesogenic, and lentogenic (Cox and Plemper, 2017; Gao et al., 2019; Neog et al., 2023). Associated clinical signs include high fever, dyspnea, dysentery, nervous disorders, and bleeding of mucous and serous membranes, causing serious financial losses in the poultry industry (Jia et al., 2018). Although there is only one known NDV serotype, existing vaccines fail to control NDV infections because there are multiple NDV genotypes, the virus evolves rapidly, and traditional vaccines often fail. Therefore, there is an urgent need to develop new strategies to prevent and control this disease.

The genome of NDV is either 15186, 15192, or 15198 nucleotides in length and contains six open reading frames encoding the nucleoprotein (NP), phosphoprotein (P), matrix protein (M), fusion protein (F), hemagglutinin-neuraminidase protein (HN), and large RNA-dependent polymerase protein (L), as well as two additional proteins, V and W, through P-gene editing (Zhang et al., 2014; Brown and Bevins, 2017). The single NDV serotype has been divided into two classes (I and II) based on whole-genome and F gene sequences (Dimitrov et al., 2016; Gao et al., 2019; Doan et al., 2022). Classes I and II can be further divided by genotype, with genotype VII being the most prevalent and involved in recent outbreaks in Europe, Africa, South America, and Asia (Desingu et al., 2016; Cox and Plemper, 2017; Mase, 2022). In China, NDV VII strains have predominated since 2000, causing high mortality in chickens and other birds, and resulting in significant yearly economic losses to the chicken industry worldwide (Zhu et al., 2016; Xiang et al., 2020).

In this study, we began with a 2017 NDV VII strain isolate from a chicken in Gannan, Gansu Province, in 2017, which provided important information. However, the characteristics of NDV VII isolates from Northwest China are not well known, and it is unclear how differences in infection can occur. Here, we focused on sequencing and biological characteristics of NDV VII

isolates from chickens and cells, which could provide a method for sequencing unknown viruses and a foundation for further viral research.

Materials and Methods

Viral isolation and sequence analysis

In total, 86 oral and cloacal swabs from Shaanxi and Gansu provinces in northwest China were analyzed. Thirteen isolates were identified as La Sota, whereas three samples had the same sequence and were classified as the NDV VII strain based on PCR. The genome of the NDV isolate was determined using next-generation sequencing (NGS), and the results were deposited in NCBI with the accession number OQ144966. The other sequences used in this study were obtained from NCBI and automatically aligned using MAFFT. A maximum likelihood tree was constructed using IQ-TREE ver. 2.1.1. Sequence diversity analysis was performed using MEGA 7.0 program. A neighbor-joining phylogenetic tree was constructed based on the NDV F gene using MEGA 7.0 with 1,000 bootstrap replicates.

Assessment of MDT, ICPI, and IVPI

The mean death time (MDT), intracerebral pathogenicity index (ICPI), and intravenous pathogenicity index (IVPI) were determined as described by Li et al. (2019a). Each viral stock dilution (10^{-1} to 10^{-10}) was inoculated based on a 0.1 ml volume into 9-day-old chicken embryos (10 each), which were incubated at 37 °C. Dead embryos were discarded within 24 h. Viability of the chicken embryos was scored once per day in the morning and evening for 10 days, and times of death were recorded to obtain MDT values. Ten 1-day-old SPF chickens were inoculated with 0.05 mL each, and 0.05 mL of sterile saline was used as a control. After inoculation, chicks were fed in a biosafety isolator and observed every 24 h for 10 d. These observations were made according to ICPI standards by de Graaf et al. (2022). Ten 6-week-old specific pathogen free (SPF) chickens were inoculated with 0.1 ml intravenously, with the same volume of sterile saline used for controls. Inoculated chickens were observed continuously for 10 d and the resulting scores used according to prescribed standards to obtain IVPIs.

Cell culture

DF-1 chicken embryo fibroblasts (DF-1), obtained from Northwest A&F University Infectious Diseases Lab, were used measure NDV pathogenicity. Cells were maintained and cultured in Dulbecco's modified Eagle's medium (DMEM; Gibco, Grand Island, NY, USA) supplemented with 10% fetal bovine serum (FBS; Hyclone, Logan, Utah, USA). All procedures were performed under 5% CO_2 and 37°C in flat-bottom plates.

Plaque assays

At 85% confluency, cells were infected with NDV at a multiplicity of infection (MOI) of 1. Cytopathic effect (CPE) was scored light microscopy at 12, 24, and 48 h. Plaque-forming units were measured as previously described at 36 h after infection at MOIs of 0.0001, 0.001, 0.01, 0.1, and 1 (Li et al., 2019b). In brief, 8×10^4 DF-1 cells were seeded into 24-well plates, 24 h prior to infection. Cells were washed three times with PBS,

300 µL viral suspension was added, and plates were incubated for 1 h. The supernatants were replaced with DMEM containing 2% FBS and 1% methyl cellulose (Solarbio, Beijing, China), and cells were incubated for an additional 3–4 days. Cells were fixed with 5% formaldehyde in PBS and stained with 1% methylene blue before counting plaques.

RNA extraction and cDNA preparation

Total RNA was extracted using the TRIzol reagent (TaKaRa, Dalian, China) according to the manufacturer's instructions. RNA concentrations were measured and diluted to 100 ng/µL; 3 µL of each RNA sample was used for cDNA preparation. Synthesis of cDNA was performed using the StarScript II First-Strand cDNA Synthesis Mix (GenStar, Beijing, China) according to the manufacturer's instructions. In brief, the reaction was performed in a volume of 20 µl, containing 500 ng total RNA, 10 µl 2× reaction mix, 1 µl oligo d(T)$_{18}$ (50 µM), 1 µl StarScript II RT Mix, and RNase-free ddH$_2$O up to 20 µl. Reaction conditions were: 25°C for 10 min, 42°C for 30 min, and 85°C for 5 min. The resulting cDNAs were stored at -20°C for further use.

Real-time quantitative PCR (RT-qPCR)

Primer sequences were (all 5′-3′): MF, CCGATCGTCCTA-CAAGACACAG; and MR, GGACGCTTCCTAGGCAGAG-CAT. The M gene was cloned and ligated into the pMD19-T vector (TaKaRa), then subjected to PCR and sequencing. The plasmid concentration was determined and 10-fold serial dilutions were used for standardization. Each DNA sample was diluted to 100 ng/µL, with 1 µL used for qPCR. The qPCR procedure was optimized using the 2×RealStar Green Power kit, according to the manufacturer's instructions (GenStar, Beijing, China). A standard curve was constructed as previously described (Cheng et al., 2018).

In vivo pathogenicity assessments

To assess NDV distribution after infection, 6-week old SPF chickens were randomly divided into two groups of five. One group was infected with 100 µL each of the NDV isolate (titer of 2^8) via intranasal and intraocular routes, and the other group was inoculated with 100 µL of saline solution in the same manner. At three days post infection (dpi), the brain, lung, trachea, thymus, esophagus, glandular stomach, gizzard, liver, spleen, heart, intestine, pancreas, cecal tonsil, bursa of Fabricius, rectum, kidney, and muscle tissues were collected and assayed using RT-qPCR. Pathological changes in the trachea, liver, spleen, and rectum were further assessed to study morphological changes after intranasal and intraocular infections.

To assess pathogenicity as a function of inoculation route, clinical disease signs, pathological changes, and viral proliferation were analyzed. Six-week-old SPF chickens were randomly divided into eight groups of five. Four groups were infected with 200 µL each of NDV (virus titer of 2^6) via intranasal, intraocular, intravenous injection, intramuscular injection, and cloacal routes, with control groups treated with saline solution in the same manner. After infection, the clinical signs were observed and recoded as shown in Table 1, every 12 h. Seven tissues (thymus, lung, bursa of Fabricius, intestine, caecum tonsil, liver, and spleen)

Table 1.   Scoring criteria

Score	Clinical signs	Pathological changes
0	No obvious signs	No obvious pathological change
1	Poor spirit, shrunken neck, somnolence, highly sensitive	Mild hyperemia and bleeding
2	Depression, closed eyes, and somnolence, low alertness, shrunken neck, lying down, diarrhea, yellowish-green or yellowish-white loose feces, breathing with obvious murmurs, weak stimulus response	Some organs obviously congested and bleeding
3	Lying on the ground, paralysis, head and neck tremors and convulsions or severe breathing difficulties, obvious neurological signs, severe diarrhea, yellow transparent watery excretions, no strong stimulus response	Obvious bleeding spots in the brain or digestive tract, obvious congestion and bleeding in the rectum and cloaca
4	Death	Obvious hemorrhagic and bleeding spots, band-like bleeding in the rectum and cloaca, enlarged cecal tonsils, and obvious hemorrhaging
5	Acute death	

were selected to assay viral loads based on different inoculation routes using RT-qPCR.

Histopathology

Tissue samples were collected at 3 dpi from multiple organs (trachea, liver, spleen, and rectum) and fixed in 10% neutral buffered formalin, then embedded in paraffin . Sections were cut at 3 μm, stained with hematoxylin-eosin (H&E), and examined by light microscopy for histological alterations.

Statistical analysis

Experiments were independently repeated at least twice. GraphPad Prism was used for statistical analyses. All data are presented as means ± standard deviation (SD). Differences were assessed using Student's *t*-test, one-way ANOVA, or multiple comparisons using GraphPad ver. 8.0.2. Differences were considered statistically significant at ****$P < 0.0001$, ***$P < 0.001$, **$P < 0.01$, and *$P < 0.05$; ns, not significant.

Results

We identified 13 isolates as La Sota strain, whereas three had the same sequence as the NDV VII strain, based on PCR. We selected one of the NDV VII strains and sequenced its genome using next-generation sequencing (NGS). The assembly, shown as a circle diagram, indicated that almost all viral sequences were identified (Fig. 1A). A maximum likelihood (ML) phylogenetic tree was constructed based on these genome sequences, which indicated that the isolated strain fit into the genotype VII NDV cluster (Fig. 1B).

Further analysis indicated that the strain belonged to VII.1.1 NDV based on its F sequences and was similar to the NDV isolate Chicken/China/Liaoning/03/2008 (KC542901.1) (Fig. 1C). Its sequence was 99% identical to that of a computer-predicted NDV isolate, KC542901.1. The proteolytic cleavage site motif for the F0 protein was ^{112}RRQKR↓F^{117}, consistent with our pathogenicity analyses. The MDT, ICPI, and IVPI values of the NDV isolate were 39.2 h, 1.91, and 2.88, respectively, indicating that it is velogenic.

To assess infectivity, DF-1 cells were infected at 0.1 MOI and observed at 12, 24, and 36 h post infection (hpi). Compared to

controls, viral infection of DF-1 cells resulted in obvious CPEs at 12, 24, and 48 hpi. Plaque assays indicated different viral loads, specifically at 0.01, 0.1, and 1 MOI. When DF-1 cells were infected with the NDV isolate, significant syncytium formation was observed, consistent with the characteristics of a velogenic virus (Fig. 2A and B).

We observed obvious bleeding in the tracheal mucosa and inflammatory cell infiltration in the trachea. The liver showed hepatocyte degeneration associated with interstitial mononuclear cellular infiltration and increased inflammatory cells. The spleen was swollen and congested, with severe hemorrhagic necrosis and fibrinous inflammation. Moreover, the rectum exhibited hemorrhaging and swelling and the mucosa showed hemorrhagic inflammation associated with exfoliation, congestion, and inflammatory cell infiltration (Fig. 3A and B). A qPCR method was used to detect [REMOVED = FIELD]NDV in chicken tissues after infection (Fig. 3C). Melting curve analysis showed a single peak, with amplification curves of plasmids with different concentrations showing regular amplification, indicating that the primers met the requirements for qPCR. We observed high viral loads in the thymus, bursa of Fabricius, intestine, liver, and spleen, but lower viral loads in the kidney, muscle, brain, and pancreas, consistent with our clinical and pathological observations (Fig. 3D).

To assess differences in clinical infections with the VII.1.1 NDV genotype, different routes of inoculation were analyzed. The first clinical signs and death occurred in the intravenously injected group of chickens, followed by the intramuscularly infected group, with the least severe disease observed with cloacal infection (80% survival) (Fig. 4A). The most severe clinical signs occurred in intravenously infected chickens: death, obvious hemorrhagic spots, blood spots, and bands of bleeding in the rectum and cloaca, as well as enlarged cecal tonsils and obvious hemorrhage 60 hpi. Cloacal infection resulted in the mildest disease, with only a few chickens exhibiting lethargy, shrunken necks, somnolence, high sensitivity, mild hyperemia, and bleeding (Fig. 4B). We chose seven tissues: thymus, liver, spleen, lung, small intestine, bursa of Fabricius, and cecum tonsil, to measure viral
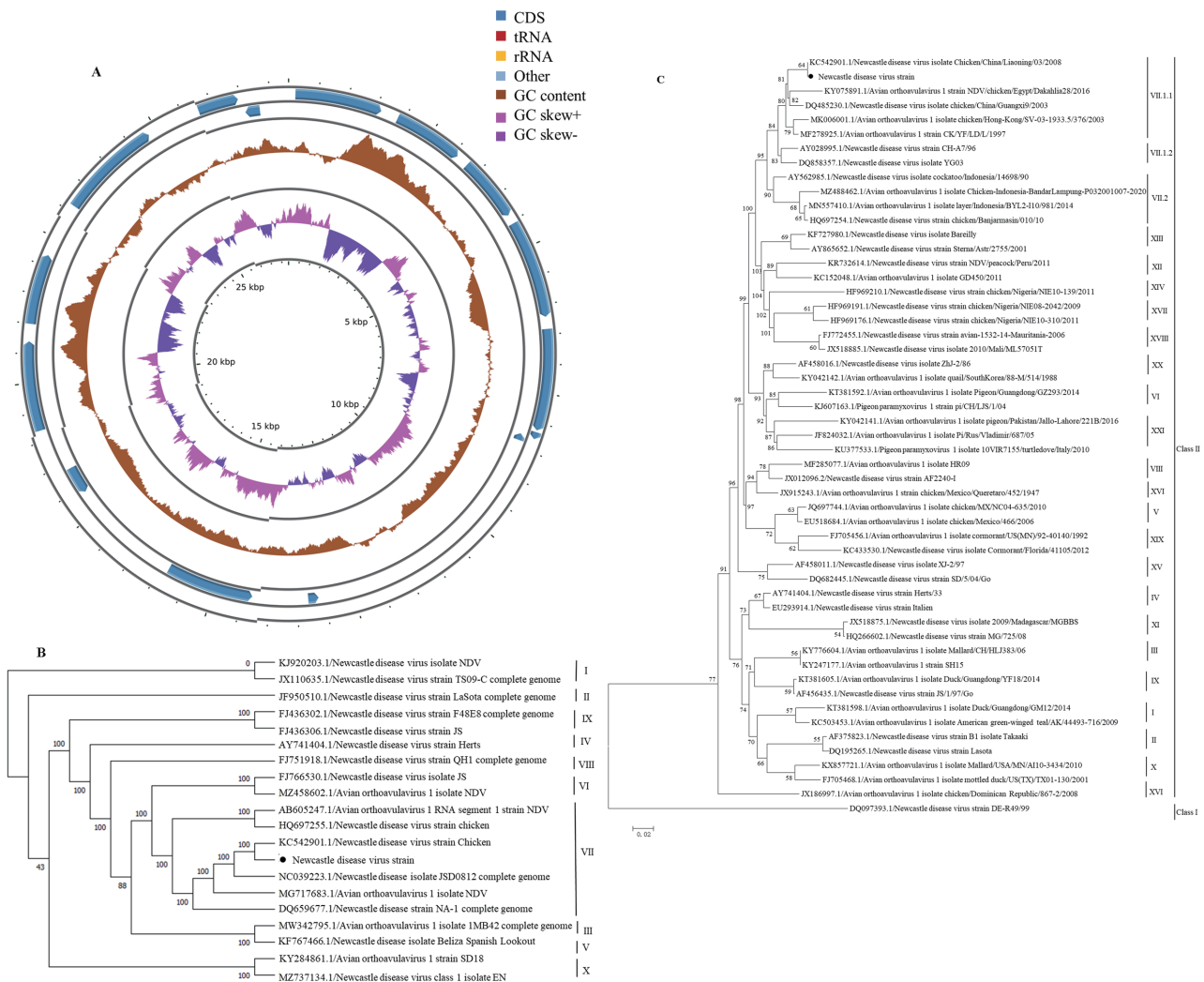
Fig. 1. **Identification and characteristics of a Newcastle disease virus (NDV) isolate.** (A) Assembly by NGS. (B) Maximum likelihood (ML) phylogenetic tree constructed using IQ-TREE with 1,000 bootstrap replicates. (C) Neighbor-joining (NJ) phylogenic tree based on NDV F using MEGA 7.0 with 1,000 bootstrap replicates. Numbers on branches indicate evolutionary distances. Our strain's sequence (black spot) aligned with those of other NDV strains obtained from GenBank of NCBI.

load as a function of route of infection. Viral loads were higher in liver, spleen, small intestine, bursa of Fabricius, and cecum tonsil after intravenous injection, while they were lower in cloacal infections, which was similar to the results of intranasal and intraocular inoculation (Fig. 4C).

Discussion

Genotype VII NDV strains predominate in China, with sub-genotype VII strains isolated from different provinces and cities throughout China, particularly in the south and southeast (Xiang et al., 2020; Chen et al., 2021). Currently, the primary methods for sequencing viral genomes are Sanger and high-throughput sequencing. We used high-throughput sequencing, which provided important information for the study of viral gene sequences and

SNPs, greatly reducing detection costs.

Our NDV strain was isolated from a chicken in Gannan, Gansu province, northwest China and was determined to have VII.1.1 genotype based on phylogenetic analysis. However, genotype VII.1.1 includes VIIb, VIId, VIIe, and VIIj (Shafaati et al., 2022); the strain isolated in this study was most similar to the VIId strain isolated from Liaoning Province in 2008. Xiang et al. revealed that eastern China is likely the transmission center of genotype VII NDVs, which have gradually spread to surrounding areas; however, these are identified relatively less frequently in the northwestern and western regions of China (Xiang et al., 2020).

To understand the epidemiological characteristics of genotype VII NDVs in China and the correlation between genotypes, it is necessary to conduct epidemiological surveillance on a national
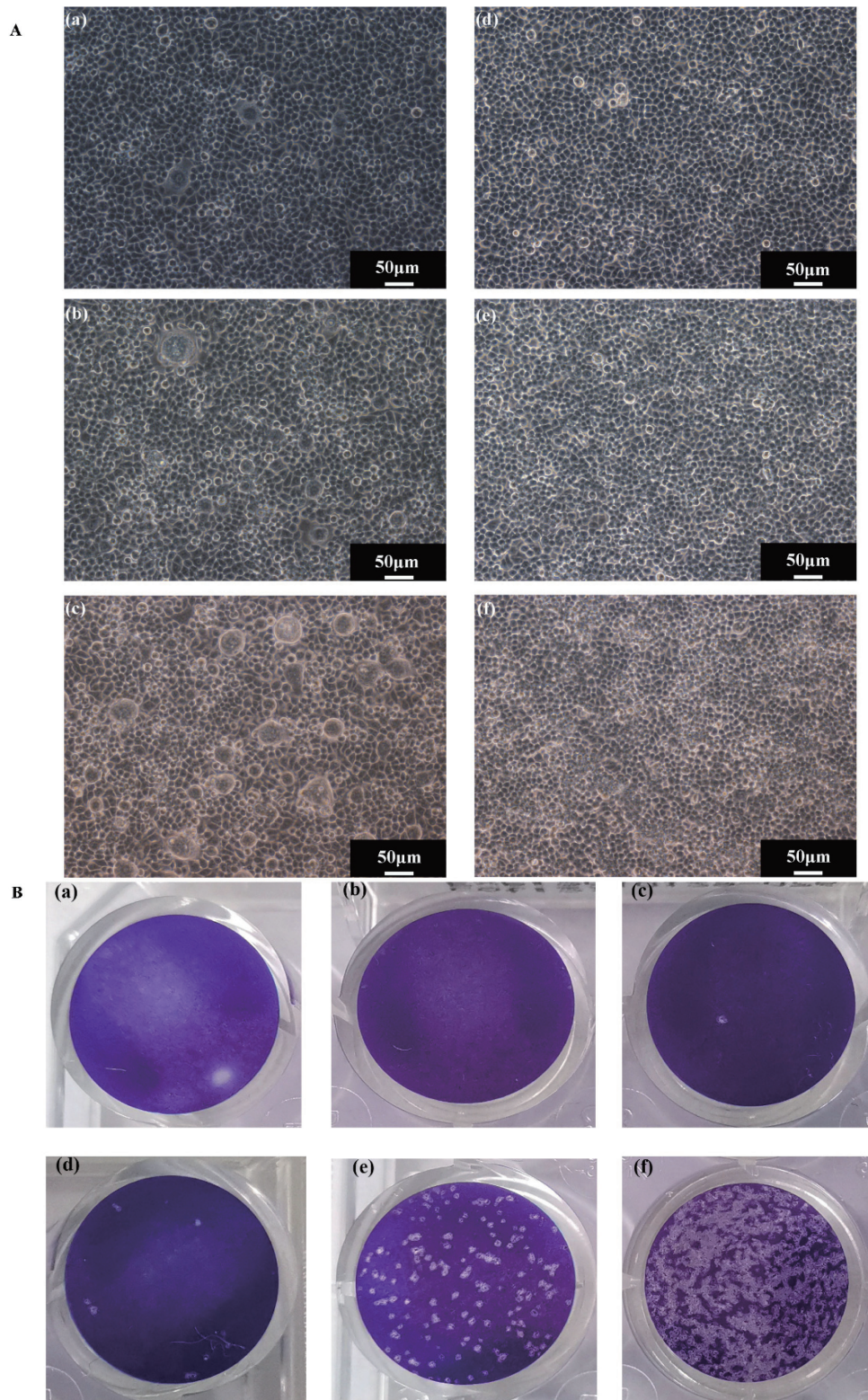
Fig. 2.   **Infection with NDV isolate.** A. DF-1 cells infected at an MOI of 0.1. (a)–(c) exhibit obvious CPE at 12, 24, and 48 hpi, whereas (d)–(f) show no effects in mock-infected control cells. Experiments were repeated at least three times and one is shown. The length of each scale bar is 50 μm. (B) Plaque-forming units counted at 36 hpi at MOIs of 0.0001, 0.001, 0.01, 0.1, and 1. (a) mock infected; (b)–(f) infected.
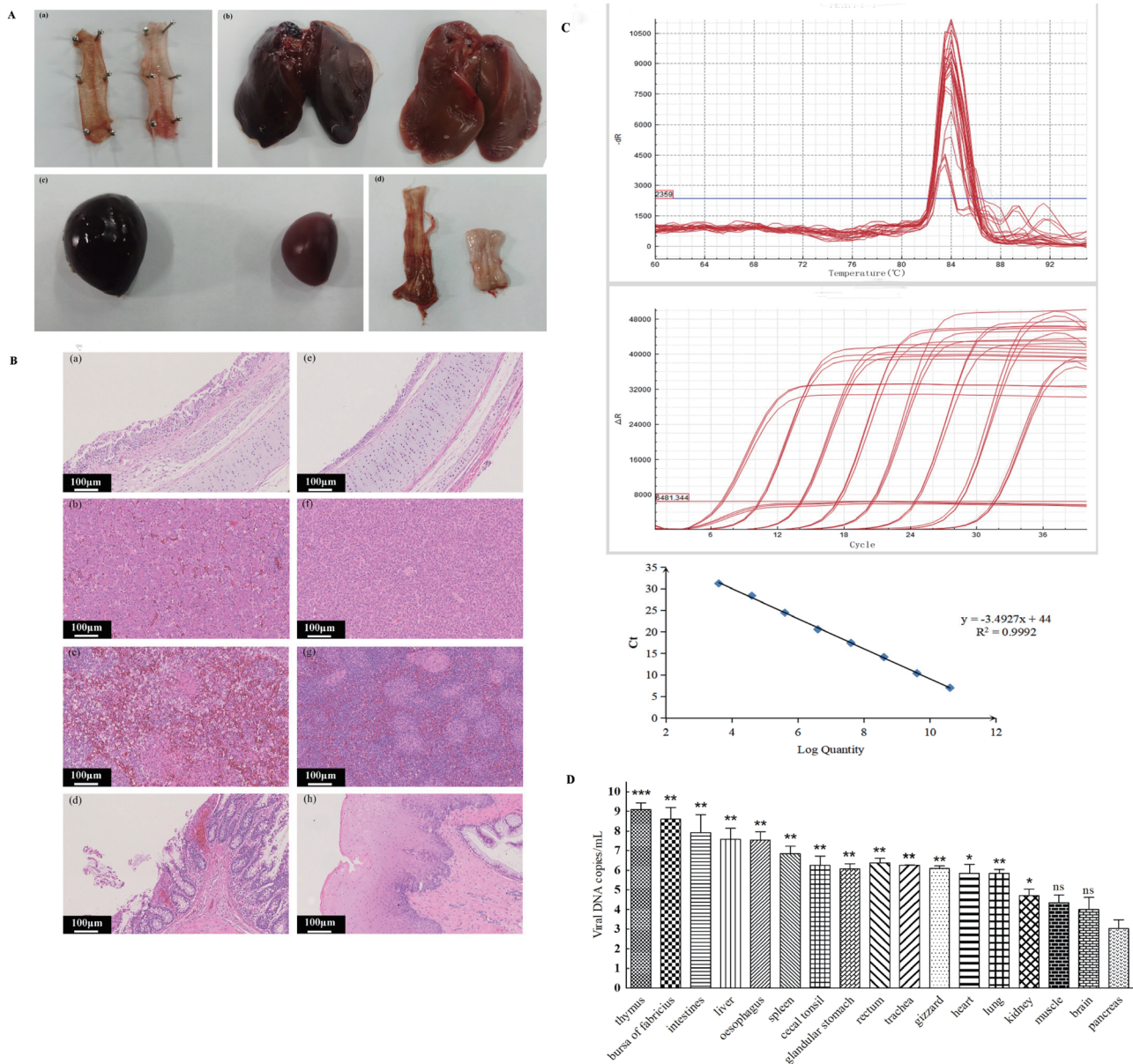
Fig. 3.   **Pathogenicity of Newcastle disease virus (NDV) strain.** (A) Pathological changes in the trachea, liver, spleen, and rectum after inoculation with NDV (2^8) or saline solution. In each panel, infected tissues are on the left and uninfected tissues are on the right. (B) Histopathology of trachea, liver, spleen, and rectum challenged with the NDV strain (a–d) and uninfected controls (e–h) (H&E, ×100). Scale bars, 100 μm. (C) Construction of qPCR method. (a) melting curves, (b) amplification curves for plasmid standards, (c) Standard curve. (D) Viral loads of. The pancreas, with the lowest expression, was used as a benchmark to compare with other organs. Data are shown as mean ± SD (n=5). Data were analyzed using GraphPad Prism using unpaired, two-tailed t-tests: *$P < 0.05$, **$P < 0.01$, and ***$P < 0.001$.

scale. The lentogenic NDV strains were distributed in almost all organs, especially the digestive and respiratory organs, in the virus-infected chicken embryo, whereas organ damage with lentogenic infection was not as severe as that with velogenic NDV (genotype VII.2). Dead embryos were observed to be hemorrhag-

ing in almost all visceral organs after genotype VII.2 NDV infection (Angeliya et al., 2022).

Previous reports have shown that NDV can be disseminated in the blood, so that virus can be detected in all tissues and organs after infection; however, the viral loads in tissues and organs have
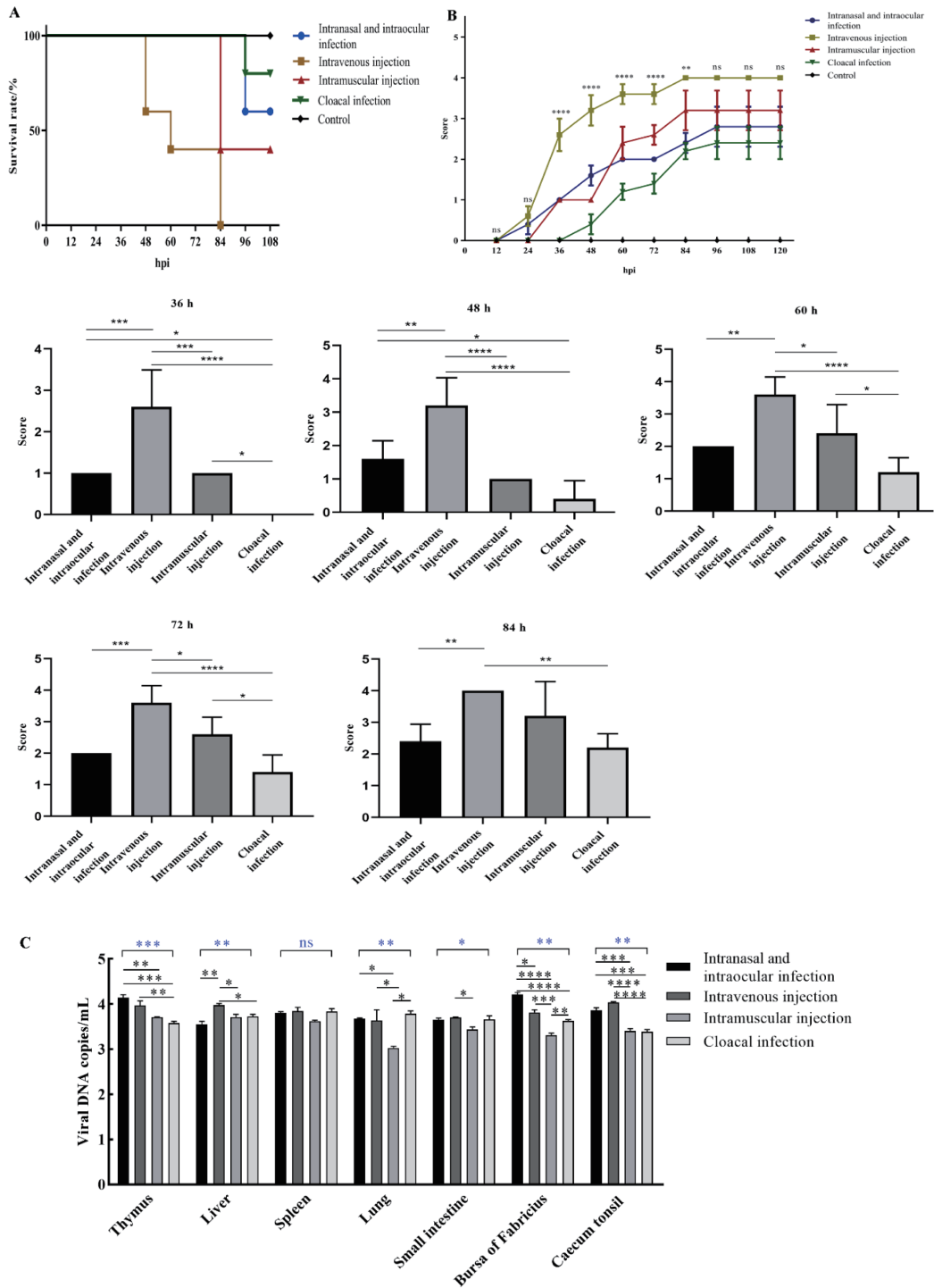
Fig. 4. **NDV pathogenesis as a function of route of infection.** (A) Survival curves for chickens infected by intranasal and intra-ocular (blue), intravenous injection (yellow line), intramuscular injection (red), cloacal (green) routes, as well as uninfected controls (black line). Survival curves were constructed using GraphPad Prism. (B) Clinical scoring of clinical signs and pathological changes. (a) Scoring performed every 12 hpi based on Date were analyzed using one-way ANOVA; (b)-(f) Time points with significant differences were analyzed using multiple comparisons. (C) Viral loads in thymus, lung, bursa of Fabricius, intestine, caecum tonsil, liver, and spleen measured by qPCR. Data are shown as mean ± SD (n=5). Data were analyzed in GraphPad Prism using one-way ANOVA (blue) or multiple comparisons (black). *$P < 0.05$, **$P < 0.01$, ***$P < 0.001$, ****$P < 0.0001$; ns, not significant.

discrepancies between NDV genotypes (Jia et al., 2022; Mao et al., 2022). We observed high viral loads in different tissues showed high levels in the thymus, bursa of Fabricius, intestine, liver, and spleen, with lower viral loads in the kidney, muscle, brain, and pancreas. This may be related to the fact that NDVs are immunosuppressive and therefore replicate to high levels in some immune organs, such as the thymus, bursa of Fabricius, and spleen. While other tissues (kidney, muscle, and pancreas) were not typical lesion areas for NDV infection, their viral loads were relatively lower. Interestingly, weak clinical neurological symptoms were observed; however, the amount of virus detected in the brain was very low, which might be related to the timing of the dissection. If chickens exhibit significant neurological symptoms, the brain may exhibit significant bleeding and increased viral load.

El-Morshidy et al. (2021) reported prominent respiratory manifestations, the highest mortality rate after intranasal inoculation, and less severe clinical manifestations and postmortem lesions after choanal inoculation, whereas features of non-purulent encephalitis were produced by intraocular inoculation. However, pathogenicity differences between routes should also be considered, and our study adds some data regarding pathogenicity as a function of route.

The M gene is the matrix protein gene of NDV, which is relatively conserved in this genotype. Therefore, we analyzed the M gene using qPCR method. Of the different inoculation routes, chickens vaccinated intravenously died most quickly without disease signs, whereas those inoculated via the intranasal and intraocular routes showed obvious signs, especially neurological ones. However, no obvious pathologies were observed in brain tissue of infected chickens, and the viral load was relatively low. This could be related to blood-brain barrier and/or peripheral nerve injury; however, the specific mechanism underlying this difference requires further study.

Viral loads of most organs after intravenous infection were slightly higher than those of other infection routes, while the viral loads of the thymus and bursa of Fabricius were significantly higher than those of other routes after intranasal and intraocular infection. This could be related to the fact that NDV is an immunorestrictive virus that may stimulate Hard's gland during intranasal and intraocular infection, which can quickly cause an immune response, so as to slow clinical death and mild lesions despite high viral loads. After infection by all routes, high viral loads were detected in all organs, which also indicated that NDVs are capable of causing systemic infection, consistent with our findings. However, the relationship between the amount of virus carried in different tissues, the time of death, and pathological changes remain to be explored by adding additional tissues and time points in the future.

In conclusion, this study revealed the evolution, pathogenicity, and cell and chicken infectivity of a genotype VII NDV strain isolated in western China. Furthermore, qPCR was used to detect genotype VII NDV based on the M gene, and viral proliferation and pathogenicity were assessed as a function of inoculation route. To better control this predominant NDV strain, more detailed analyses of its biological properties and pathogenic characteristics with different genotypes and routes of infection are urgently needed.

Ethics Statement

The experiments using chickens in this study were performed strictly according to guidelines of the Committee for the Ethics of Animal Care and Experiments at Yangling Vocational & Technical College (approval number 2021YZ060920-012, September 20, 2021).

Acknowledgements

Author Contributions

Q.X.X. performed experiments, analyzed data, and wrote the first draft of the manuscript. J.Y.Q. designed the study, analyzed data, and reviewed the manuscript. Z.Z.C. collected samples, provided data, and reviewed the manuscript. F.X.L. collected samples and performed experiments. W.W.H. supervised experiments, designed the study, and reviewed the manuscript.

Conflicts of Interest

The authors declare no conflict of interest.

References

Angeliya L, Kristianingrum YP, Asmara W and Wibowo MH. Genetic characterization and distribution of the virus in chicken embryo tissues infected with Newcastle disease virus isolated from commercial and native chickens in Indonesia. Veterinary World, **15**: 1467–1480. 2022. https://doi.org/10.14202/vetworld.2022.1467-1480, PMID:35993083

Brown VR and Bevins SN. A review of virulent Newcastle disease viruses in the United States and the role of wild birds in viral persistence and spread. Veterinary Research, **48**: 68-83. 2017. https://doi.org/10.1186/s13567-017-0475-9, PMID:29073919

Chen X, Chen S, Chen H, Tian J, Zhao X, Jia Y, Xiao S, Wang X, Liu H and Yang Z. Comparative biology of two genetically closely related Newcastle disease virus strains with strongly contrasting pathogenicity. Veterinary Microbiology, **253**: 108977. 2021. https://doi.org/10.1016/j.vetmic.2020.108977, PMID:33421684

Cox RM and Plemper RK. Structure and organization of paramyxovirus particles. Current Opinion in Virology, **24**: 105–114. 2017. https://doi.org/10.1016/j.coviro.2017.05.004, PMID:28601688

Cheng W, He X, Jia H, Chen G, Wang C, Zhang J and Jing Z. Development of a SYBR Green I real-time PCR for detection and quantitation of orthopoxvirus by using Ectromelia virus. Molecular and Cellular Probes, **38**: 45–50. 2018. https://doi.org/10.1016/j.mcp.2017.12.001, PMID:29224776

de Graaf JF, van Nieuwkoop S, de Meulder D, Lexmond P, Kuiken T, Groeneveld D, Fouchier RAM and van den Hoogen BG. Assessment of the virulence for chickens of Newcastle Disease virus with an engineered multi-basic cleavage site in the fusion protein and disrupted V protein gene. Veterinary Microbiology, 269:109437. 2022.

Desingu PA, Singh SD, Dhama K, Vinodhkumar OR, Barathidasan R, Malik YS, Singh R and Singh RK. Molecular characterization, isolation, pathology and pathotyping of peafowl (*Pavo cristatus*) origin Newcastle disease virus isolates recovered from disease outbreaks in three states of India. Avian Pathology, **45**: 674–682. 2016. https://doi.org/10.1080/03079457.2016.1198005, PMID:27724072

Doan PTK, Low WY, Ren Y, Tearle R and Hemmatzadeh F. Newcastle disease virus genotype VII gene expression in experimentally infected birds. Scientific Reports, **12**: 5249. 2022. https://doi.org/10.1038/s41598-022-09257-y, PMID:35347193

Dimitrov KM, Ramey AM, Qiu X, Bahl J and Afonso CL. Temporal, geographic, and host distribution of avian paramyxovirus 1 (Newcastle disease virus). Infection, Genetics and Evolution, **39**: 22–34. 2016. https://doi.org/10.1016/j.meegid.2016.01.008, PMID:26792710

El-Morshidy Y, Abdo W, Elmahallawy EK, Abd EL-Dayem GA, El-Sawak A, El-Habashi N, Mosad SM, Lokman MS, Albrakati A and Abou Asa S. Pathogenesis of Velogenic Genotype VII.1.1 Newcastle Disease Virus Isolated from Chicken in Egypt via Different Inoculation Routes: Molecular, Histopathological, and Immunohistochemical Study. Animals (Basel), **11**: 3567. 2021. https://doi.org/10.3390/ani11123567, PMID:34944344

Gao S, Zhao Y, Yu J, Wang X, Zheng D, Cai Y, Liu H and Wang Z. Comparison between class I NDV and class II NDV in aerosol transmission under experimental condition. Poultry Science, **98**: 5040–5044. 2019. https://doi.org/10.3382/ps/pez233, PMID:31064012

Jia YQ, Wang XL, Wang XW, Yan CQ, Lv CJ, Li XQ, Chu ZL, Adam F, Xiao S, Zhang SX and Yang ZQ. Common microRNA-mRNA Interactions in Different Newcastle Disease Virus-Infected Chicken Embryonic Visceral Tissues. International Journal of Molecular Sciences, **19**: 1291. 2018. https://doi.org/10.3390/ijms19051291, PMID:29693643

Jia YQ, Wang XW, Chen X, Qiu XX, Wang XL and Yang ZQ. Characterization of chicken *IFI35* and its antiviral activity against Newcastle disease virus. Journal of Veterinary Medical Science, **84**: 473–483. 2022. https://doi.org/10.1292/jvms.21-0410, PMID:35135934

Li PY, Gao JP, Zhao LL, Tian Y, Xu MJ, Wang CL and Xu T. Isolation,identification and pathogenicity of a Newcastle disease virus isolate from racing pigeon. Heilongjiang Animal Science and Veterinary Medicine, **14**: 151–154. 2019a.

Li X, Jia Y, Liu H, Wang X, Chu Z, Hu R, Ren J, Xiao S, Zhang S, Wang X and Yang Z. High level expression of ISG12(1) promotes cell apoptosis via mitochondrial-dependent pathway and so as to hinder Newcastle disease virus replication. Veterinary Microbiology, **228**: 147–156. 2019b. https://doi.org/10.1016/j.vetmic.2018.11.017, PMID:30593361

Mao Q, Ma S, Schrickel PL, Zhao P, Wang J, Zhang Y, Li S and Wang C. Review detection of Newcastle disease virus. Frontiers in Veterinary Science, **9**: 936251. 2022. https://doi.org/10.3389/fvets.2022.936251, PMID:35982920

Mase M. Hemagglutinin-neuraminidase gene of genotype VII Newcastle disease virus strains isolated in Japan. Journal of Veterinary Medical Science, **84 :1-5.** 2022. https://doi.org/10.1292/jvms.21-0490, PMID:34789612

Neog S, Kumar S and Trivedi V. Isolation and characterization of Newcastle disease virus from biological fluids using column chromatography. Biomedical Chromatography, **37**: e5527. 2023. https://doi.org/10.1002/bmc.5527, PMID:36250786

Shafaati M, Ghorbani M, Mahmodi M, Ebadi M and Jalalirad R. Molecular evaluation and genetic characterisation of Newcastle disease virus's haemagglutinin-neuraminidase protein isolated from broiler chickens in Iran. Veterinary Medicine and Science, **8**: 219–228. 2022. https://doi.org/10.1002/vms3.629, PMID:34606181

Wang Z, Zhao X, Wang Y, Sun C, Sun M, Gao X, Jia F, Shan C, Yang G, Wang J, Huang H, Shi C, Yang W, Qian A, Wang C and Jiang Y. In Vivo Production of HN Protein Increases the Protection Rates of a Minicircle DNA Vaccine against Genotype VII Newcastle Disease Virus. Vaccines, **9**: 723. 2021. https://doi.org/10.3390/vaccines9070723, PMID:34358140

Xiang B, Chen L, Cai J, Liang J, Lin Q, Xu C, Ding C, Liao M and Ren T. Insights into Genomic Epidemiology, Evolution, and Transmission Dynamics of Genotype VII of Class II Newcastle Disease Virus in China. Pathogens (Basel, Switzerland), **9**: 837. 2020. https://doi.org/10.3390/pathogens9100837, PMID:33066232

Zhang Y, Shao M, Yu X, Zhao J and Zhang G. Molecular characterization of chicken-derived genotype VIId Newcastle disease virus isolates in China during 2005–2012 reveals a new length in hemagglutinin–neuraminidase. Infection, Genetics and Evolution, **21**: 359–366. 2014. https://doi.org/10.1016/j.meegid.2013.12.003, PMID:24333370

Zhu J, Hu S, Xu H, Liu J, Zhao Z, Wang X and Liu X. Characterization of virulent Newcastle disease viruses from vaccinated chicken flocks in Eastern China. BMC Veterinary Research, **12**: 113. 2016. https://doi.org/10.1186/s12917-016-0732-6, PMID:27305943